scientific reports

Check for updates

OPEN

Predicting outcomes in patients with sepsis-associated encephalopathy using prefrontal functional connectivity analysis

Tae Jung Kim[1,2], Jae-Myoung Kim[3], Ji Sung Lee[5], Soo-Hyun Park[6], Jihyun Cha[3], Hyeon-Min Bae[3,4] & Sang-Bae Ko[1,2]✉

We investigated the relationship between prefrontal functional connectivity of oxyhemoglobin and outcomes in sepsis-associated encephalopathy (SAE). Additionally, we developed a prognostic method for patients with SAE. A total of 40 consecutive patients with SAE were prospectively included. Cerebral oxyhemoglobin data were obtained using functional near-infrared spectroscopy. Functional connectivity such as density was evaluated as the strength of the temporal correlation between channels based on Pearson's correlation coefficient of oxyhemoglobin. We obtained clinical information and evaluated severity scores using Acute Physiology and Chronic Health Evaluation (APACHE) III. Outcomes were evaluated using the modified Rankin Scale (mRS) at discharge. Patients were categorized into two groups: good outcome (mRS 0–3), and poor outcome (mRS 4–6). Among the patients with SAE, 17 (42.5%) had good outcomes. Regarding connectivity analysis, density values were significantly higher in good outcome groups at all threshold values. The developed predictive method of good outcomes using the density value at a threshold of 0.6 and the APACHE III score showed very good predictive power (area under the curve 0.951 [95% confidence interval 0.893–1.00]). This method had better discrimination powers for predicting outcome than density had at 0.6 (0.716 [0.557–0.876]; $P = 0.04$) or the APACHE III score had alone (0.857 [0.735–0.979]; $P = 0.09$). A higher functional connectivity value of oxyhemoglobin in the prefrontal connectivity analysis was associated with good outcomes in SAE. Functional connectivity analysis of the prefrontal cortex and sepsis severity may help predict the prognosis in SAE patients.

Keywords Sepsis, Sepsis-associated encephalopathy, Patient outcome assessment, APACHE, Spectroscopy, Near-infrared

Sepsis is a critical medical condition caused by the host response to an infection, resulting in extensive systemic inflammation or failure of multiple organs[1–5]. Neurological manifestations of sepsis range from delirium or altered mental status to focal neurological dysfunction, seizure, or coma[6–9]. This acute encephalopathy, occurring in a course of sepsis, is called sepsis-associated encephalopathy (SAE), and is often related with poor clinical outcomes[3,6–8]. The underlying mechanisms of SAE are poorly understood and include a complex interplay of inflammatory responses, microscopic brain injury, disruption of the blood–brain barrier (BBB), compromised cerebral microcirculation, and infection-induced changes in brain metabolism[7–14]. Despite SAE being associated with a poor prognosis and increased mortality risk, its diagnosis is challenging, primarily depending on clinical assessments and ruling out other causes of altered mental states. Moreover, no reliable methods exist to accurately assess the prognosis of SAE. In practice, no diagnostic method can differentiate between patients who recover and those who remain unconscious. This is crucial for managing patients with sepsis; however, the absence of reliable prognostic markers for SAE limits timely decision-making in its treatment.

[1]Department of Neurology, Seoul National University, College of Medicine, 101 Daehak-ro, Jongno-gu, Seoul 03080, Republic of Korea. [2]Department of Critical Care Medicine, Seoul National University Hospital, Seoul, Republic of Korea. [3]Department of Research and Development, Optics Brain Electronics Laboratory, OBELAB Inc., Seoul, Republic of Korea. [4]Department of Electrical Engineering, Korea Advanced Institute of Science and Technology, Daejeon, Republic of Korea. [5]Clinical Research Center, Asan Medical Center, Seoul, Republic of Korea. [6]Department of Neurology, Soonchunhyang University Seoul Hospital, Seoul, Korea. ✉email: sangbai1378@gmail.com

Functional near-infrared spectroscopy (fNIRS) is a non-invasive, high-resolution method for continuous monitoring that enables the measurement of oxyhemoglobin and deoxyhemoglobin levels in the prefrontal cortex[15]. fNIRS offers enhanced spatial resolution for quantifying oxyhemoglobin and deoxyhemoglobin levels, which are associated with the blood-oxygen-level-dependent signal observed in functional magnetic resonance imaging. This technique can provide valuable insights into regional cerebral hemodynamics, including cerebral microcirculation and fluctuations in cerebral blood flow. Among the various types of analysis methods for the fNIRS modality, connectivity analysis evaluates the functional relationships within the brain[16]. Using connectivity analysis, previous studies have shown that task-based functional connectivity, which assesses brain activity in response to specific stimuli or challenges, is reduced in individuals with Alzheimer's disease, major depressive disorder, and attention-deficit/hyperactivity disorder[17–19]. Moreover, recent studies suggested that resting-state functional connectivity[20], measuring inherent fluctuation of the brain activity, was impaired in patients with altered mentality in a consciousness-level dependent manner[21].

In our study, we deliberately chose a resting-state approach to avoid performing tasks from patients with SAE. Therefore, the aim of this study was to explore whether a decrease in functional connectivity, as determined by fNIRS, is associated with outcomes in SAE. Additionally, we developed a method for predicting outcomes in SAE.

Methods

Study population

We initially evaluated 48 patients with SAE who were admitted to the intensive care unit (ICU) and assessed by neurointensivists in our hospital between June 2016 and February 2021. The inclusion criteria were (1) age ≥ 18 years; (2) sepsis diagnosed according to Sepsis-3 definition[3]; (3) SAE diagnosed with cerebral dysfunction (Glasgow Coma Scale [GCS] ≤ 14 or with delirium) caused by systemic responses to infections without structural abnormality, cerebral nervous system infection, and encephalopathy due to other causes such as hepatic, uremic, and toxic[7–9,22]. Moreover, fNIRS monitoring was performed using a wireless continuous-wave near-infrared spectroscopy (CW-NIRS) system (NIRSIT, OBELAB Inc., Seoul, Republic of Korea) considering the clinical stability of the patients with sepsis[17–23].

Baseline characteristics and clinical information

We obtained demographic data on age, sex, and comorbidities such as vascular risk factors and cancer. We collected clinical information related to sepsis, including infection sites, antimicrobial medications and duration of antimicrobial treatment, sedation during monitoring, laboratory findings including levels of procalcitonin (PCT), high-sensitivity C-reactive protein (hs-CRP), white blood cell (WBC) count, percentage of segmented neutrophils (%), cumulative fluid input and output, cumulative fluid balance, and severity of disease, using Acute Physiology and Chronic Health Evaluation (APACHE) III[1,24,25] and the Sepsis-related Organ Failure Assessment (SOFA)[2,3,26] during NIRSIT monitoring. Serum lactate levels, body temperature, mean arterial pressure (MAP), and partial arterial pressure of oxygen during NIRSIT monitoring were also measured. Neurological assessment was performed using the GCS at the time of monitoring and discharge[27]. In addition, neurological outcomes were evaluated using the modified Rankin Scale (mRS) at discharge. We categorized the outcomes as either good or poor on the mRS as follows: 0–3, good outcome; 4–6, poor outcome[28,29].

fNIRS measurement and data processing

fNIRS signals were recorded for a minimum of 5 min in the supine position on the prefrontal region (PFC), covering Brodmann regions that include dorsolateral-PFC, ventrolateral-PFC, frontopolar-PFC, and orbitofrontal-PFC of the participant (Fig. 1) after ensuring that the monitoring time was sufficient for data validity. The median time to monitoring after ICU admission was 3 days (interquartile range [IQR]: 2–8 days) utilizing wireless CW-NIRS system. The fNIRS monitoring system measures hemodynamic variations using two wavelengths of near-infrared light (780 nm and 850 nm) and utilizes 24 laser sources and 32 detectors to measure 48 channels of cerebral hemodynamics, with a 3-cm source-detector separation[30,31] (Fig. 1).

Connectivity analysis

Among the 48 patients included, fNIRS data were successfully collected and analyzed for 40 patients. To ensure accuracy, we visually inspected all the raw data, and any data where over 20% of the channels showed an abrupt shift greater than 20% from the initial value within 0.5 s—likely caused by motion artifacts due to contact loss from the scalp during the measurement—were excluded from further analysis[32,33]. With the aforementioned exclusion criteria, data from 8 patients were excluded due to poor signal quality. Light signals were processed using a discrete cosine transform-based bandpass filter (0.005–0.05 Hz) to eliminate cardiovascular interference and external noise. Channels with signal-to-noise ratios < 30 dB were excluded prior to extracting hemodynamic data to avoid potential data misinterpretation. Hemodynamic responses were calculated using the modified Beer–Lambert method. Finally, data from each channel were corrected for motion artifacts by regressing out the head angle changes, measured by the integrated motion sensor in NIRSIT[34]. To investigate functional connectivity, we assessed the temporal correlation strength between hemodynamic responses of all channel pairs[20,35,36]. Prefrontal correlation coefficients of oxyhemoglobin were computed for all pairwise combination of channels to ascertain overarching representative network measures from the Graph theory, such as density, clustering coefficient, and global efficiency[37,38]. A threshold value[39] was used to objectively evaluate the functional connectivity by disregarding correlations below a threshold value of 0.5, indicating weak and non-significant connections. The threshold value ranged from 0.5 to 0.9, increasing in 0.1 increments so that we could analyze the each network as function of the threshold. Correlations exceeding the threshold were designated a value of 1, resulting in the creation of a binary adjacency matrix at each threshold level[20,35,36]. Three fundamental global

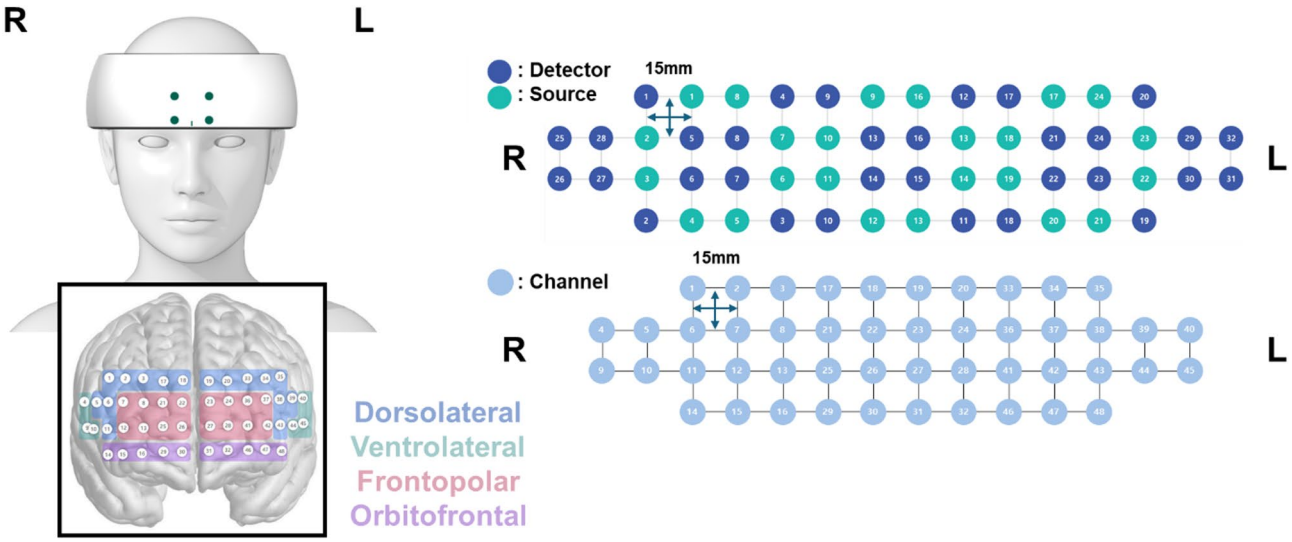

Fig. 1. Visualization of the fNIRS system on the forehead and source-detector array with channel positions.

connectivity metrics—density, clustering coefficient, and global efficiency—were subsequently computed using each threshold value[20,35,36].

Density is the ratio of existing edges to all possible edges as a fraction of the nodes above the threshold value[20,36]. The clustering coefficient is the fraction of its neighbors, which are also neighbors of each other, that is, the number of triangles around a given node that is above the threshold value[20,36]. Global efficiency is the average inverse shortest path length between all pairs of nodes above a threshold value[20,36].

Data processing and analysis were conducted using MATLAB 2023b (MathWorks, Inc., Natick, MA), with network metrics extracted using the brain connectivity toolbox incorporated within MATLAB[37].

Statistical analysis

Continuous variables were assessed utilizing either Student's t-test or the Mann–Whitney U test; categorical variables were evaluated using Pearson's chi-square test or Fisher's exact test, as appropriate. In the connectivity analysis as three correlation coefficients, a comparison was conducted across the two groups (good and poor outcomes). Logistic regression was employed to estimate predicted probabilities of outcomes by integrating the correlation coefficient value and severity scores, where severity scores, such as APACHE III and SOFA scores, were utilized as indicators of outcome in patients with sepsis. A prognostic model was developed using multiple logistic regression, considering the correlation coefficient of oxyhemoglobin and severity scores. The predictive performance of the model was assessed using receiver operating characteristic (ROC) curve analysis, which involved computing the area under the curve (AUC). ROC curve analysis was used to ascertain the optimal cutoff point for prediction, which was identified based on the highest combined sensitivity and specificity, as indicated by the Youden index[40]. AUC comparisons were performed using the DeLong method[41]. Statistical analyses were performed by a medical statistician, J. S. Lee, who considered P-values < 0.05 as indicative of statistical significance. Analyses were conducted using statistical software packages, including Statistical Package for Social Sciences (version 27.0; IBM Statistics), SAS 9.4 (SAS Institute Inc.), and GraphPad Prism (version 10.1; GraphPad Software).

Ethics

This study was approved by Institutional Review Board of Seoul National University Hospital (IRB Number: H-1605-092-762) and was performed in accordance with the regulation of the Declaration of Helsinki and guidelines. The consents were obtained from patients or their family members.

Results

Baseline characteristics and clinical information

Among the 40 patients examined (mean age, 70.8 years; male sex, 57.5%), 17 (42.5%) showed good outcomes at discharge. Comorbidities did not differ between patients with good and poor outcomes (Table 1). Regarding the sources of sepsis, biliary, gastrointestinal, and genitourinary infections were more common in patients with good outcomes. However, the respiratory origin was more prevalent (47.8%) in those with poor outcomes ($P = 0.03$). However, the choice of antibiotic did not differ between the two groups. The laboratory findings, antimicrobial treatments, and cumulative fluid balances did not differ between the two groups, as presented in Table 1. The median GCS scores were notably lower in the poor outcome group than in the good outcome group during fNIRS monitoring (8 vs. 13, $P = 0.001$) and at discharge (3 vs. 15, $P < 0.001$; Table 1). Likewise, the severity of illness was assessed using APACHE III and SOFA scores, and the good outcome group had lower scores than the poor outcome group: APACHE III (81 [IQR 61–98.5] vs. 123 [109–137], $P < 0.001$) and SOFA (6 [5.5–11]

	Total (n = 40)	Good outcome (n = 17, 42.5%)	Poor outcome (n = 23, 57.4%)	*P*-value
Age, mean (SD)	70.8 ± 12.3	72.1 ± 10.0	69.2 ± 13.8	0.46
Male, n (%)	23 (57.5)	9 (52.9)	14 (60.9)	0.75
HT, n (%)	14 (35.0)	8 (47.1)	6 (26.1)	0.20
DM, n (%)	18 (45.0)	11 (64.7)	7 (30.4)	0.05
AF, n (%)	5 (12.5)	3 (17.6)	2 (8.7)	0.63
CAD, n (%)	9 (22.5)	4 (23.5)	5 (21.7)	1.00
Previous stroke/TIA, n (%)	8 (20.0)	5 (29.4)	3 (13.0)	0.25
Malignancy, n (%)	23 (57.5)	9 (52.9)	14 (60.9)	0.75
Initial GCS, median (IQR)	10 (7–12.75)	13 (9.5–14)	8 (6–10)	0.001
F/U GCS median (IQR)	10.5 (3–14.0)	15 (14–15)	3 (3–3)	< 0.001
Origins of sepsis, n (%)				0.03
Respiratory	13 (32.5)	2 (11.8)	11 (47.8)	
Biliary	5 (12.5)	3 (17.6)	2 (8.7)	
Gastrointestinal	8 (20.0)	6 (35.3)	2 (8.7)	
Genitourinary	6 (15.0)	4 (23.5)	2 (8.7)	
Others	8 (20.0)	2 (11.8)	6 (26.1)	
Antibiotics, n (%)				0.43
Glycopeptides + Carbapenem	9 (22.5)	2 (11.8)	7 (30.4)	
Carbapenem	13 (32.5)	8 (47.1)	5 (21.7)	
Glycopeptides	5 (12.5)	2 (11.8)	3 (13.0)	
Piperacillin/tazobactam or with quinolone	5 (12.5)	3 (17.6)	2 (8.7)	
Cephalosporin	3 (7.5)	1 (5.9)	2 (8.7)	
Others	5 (12.5)	1 (5.9)	4 (17.4)	
Duration of antibiotics, mean (SD), days	4.0 (3.2)	3.3 (2.7)	4.6 (2.5)	0.22
Sedation, n (%)	4 (10.0)	2 (11.8)	2 (8.7)	1.00
APACHE III score, median (IQR)	108.5 (79.5–133.5)	81 (51–98.5)	123 (109–137)	< 0.001
SOFA, median (IQR)	12.5 (9–15)	6 (5.5–11)	15 (12–17)	< 0.001
Lactic acid, mean (SD), mmol/L	4.1 (3.9)	2.5 (1.7)	5.4 (4.6)	0.01
WBC, mean (SD) $X10^3$/ul	19.9 (9.4)	20.7 (9.0)	19.3 (9.8)	0.65
Seg. Neutrophil mean, (SD), %	84.9 (16.1)	85.3 (10.9)	84.6 (19.2)	0.89
hs-CRP, mean (SD), mg/dl	27.2 (10.3)	26.2 (10.9)	27.9 (10.1)	0.61
PCT, mean (SD), ng/ml	22.6 (22.4)	26.5 (30.5)	20.6 (17.7)	0.56
Cumulative fluid input, mean (SD), ml	16,852.5 (13,615.0)	14,685.8 (13,012.1)	18,454.0 (14,112.4)	0.39
Cumulative fluid output, mean (SD), ml	14,511.1 (13,197.4)	12,392.8 (11,660.5)	16,076.7 (14,277.4)	0.39
Cumulative I/O balance, mean (SD), ml	2,341.5 (4,039.4)	2,292.9 (3,385.8)	2,377.3 (4,537.0)	0.95
BT, mean (SD), °C	37.6 (1.1)	38.0 (0.5)	37.4 (1.4)	0.054
MAP, mean (SD), mmHg	77.0 (14.2)	85.7 (15.0)	72.4 (10.7)	0.002
PaO2, mean (SD), mmHg	91.0 (30.8)	95.8 (23.9)	87.4 (35.2)	0.41
Time to fNIRS after Admission, median (IQR), d	3 (2–8)	2 (2–7)	6 (2–9)	0.15

Table 1. Baseline characteristics of included patients. SD: standard deviation; HT: hypertension; DM: diabetes mellitus; AF: atrial fibrillation; CAD: coronary artery disease; GCS: Glosgow Coma Scale; NIHSS: National Institute of Health Stroke Scale; IQR: interquartile ranges; WBC: white blood cell; seg.: segmented; hs-CRP: high-sensitivity C-reactive protein; PCT: procalcitonin; BT: body temperature; APACHE II: Acute Physiology And Chronic Health Evaluation III; SOFA: Sequential Organ Failure Assessment; MAP: mean arterial pressure; fNIRS: functional near-infrared spectroscopy.

vs. 15 [12–17], $P < 0.001$). The poor outcome group had higher serum lactate levels and a lower MAP than the good outcome group. The time to fNIRS monitoring after ICU admission did not differ between the two groups.

Connectivity analysis using fNIRS data

The hemodynamic correlation of oxyhemoglobin was assessed in prefrontal pairs of channels using Pearson's correlation coefficient for each threshold within the two distinct groups (good outcome, and poor outcome). Density values were higher in the good outcome group. The poor outcome group had the lowest density values at all threshold levels (Supplementary Fig. 1 and Table 2). Moreover, most significant differences were identified between the good and poor outcome groups using density values at a threshold of 0.5. Regarding other connectivity parameters, global efficiency was significantly different only at a threshold level of 0.5 and clustering

	Total (n = 40)	Good outcome (n = 17)	Poor outcome (n = 23)	*P*-value
Density (Pearson correlation > threshold value), mean (SD)				
0.5	0.30 ± 0.11	0.35 ± 0.13	0.26 ± 0.07	0.012
0.6	0.23 ± 0.11	0.28 ± 0.13	0.20 ± 0.07	0.013
0.7	0.16 ± 0.10	0.20 ± 0.13	0.13 ± 0.06	0.022
0.8	0.130 ± 0.08	0.13 ± 0.10	0.07 ± 0.04	0.050
0.9	0.03 ± 0.04	0.05 ± 0.05	0.02 ± 0.02	0.033
Global efficiency, mean (SD)				
0.5	0.56 ± 0.08	0.60 ± 0.09	0.54 ± 0.06	0.010
0.6	0.46 ± 0.10	0.49 ± 0.12	0.44 ± 0.08	0.088
0.7	0.34 ± 0.11	0.38 ± 0.13	0.32 ± 0.09	0.110
0.8	0.20 ± 0.12	0.24 0.15	0.17 ± 0.09	0.075
0.9	0.08 ± 0.09	0.11 ± 0.12	0.06 ± 0.05	0.087
Clustering coefficient, mean (SD)				
0.5	0.70 ± 0.08	0.73 ± 0.08	0.67 ± 0.07	0.012
0.6	0.64 ± 0.09	0.68 ± 0.08	0.62 ± 0.09	0.021
0.7	0.56 ± 0.11	0.58 ± 0.11	0.54 ± 0.10	0.223
0.8	0.44 ± 0.14	0.48 ± 0.13	0.40 ± 0.13	0.049
0.9	0.25 ± 0.14	0.30 ± 0.14	0.21 ± 0.14	0.051

Table 2. Connectivity value according to outcomes. SD: standard deviation.

Univariate analysis	OR (95% CI)	*P* value
Density 05 (per 0.1 unit increase)	2.76 (1.12–6.81)	0.03
Density 06 (per 0.1 unit increase)	2.71 (1.10–6.67)	0.03
Density 07 (per 0.1 unit increase)	2.87 (1.04–7.91)	0.04
Density 08 (per 0.01 unit increase)	1.15 (1.00–1.32)	0.04
Density 09 (per 0.01 unit increase)	1.31 (0.99–1.72)	0.06
APACHE III (10 unit increase)	0.59 (0.43–0.81)	0.001
SOFA (1 unit increase)	0.62 (0.47–0.81)	0.001

Table 3. Association between good outcome and connectivity analysis with sepsis severity. OR: odds ratio. *P* value by logistic regression.

coefficients at thresholds of 0.5, 0.6, and 0.8; the good outcome group was significantly higher than the poor outcome group (Supplementary Fig. 1 and Table 2).

Development of a prognostication model for SAE outcomes

Based on findings of the connectivity analysis, we examined the relationship between density and favorable outcomes (Table 3). Additionally, a prediction method was devised for SAE outcomes by using a density threshold value of 0.6 and APACHE III based on the statistical significance and density values (Table 4). The study evaluated the predictive accuracy of density at a threshold of 0.6 and the APACHE III score in forecasting discharge outcomes using ROC curves. This analysis included AUC evaluation as presented in Table 4 and Fig. 2. The AUC for density at a 0.6 threshold was 0.716 (95% confidence interval [CI], 0.557–0.876). The APACHE III model demonstrated an AUC of 0.857 (95% CI, 0.735–0.979) for predicting good outcomes at discharge (Table 4 and Fig. 2). Nevertheless, the difference in AUC values between density at the 0.6 threshold and APACHE III was not significant ($P = 0.23$; Fig. 2A). To increase the power for forecasting SAE outcomes, we combined clinical severity score and information on connectivity using multivariate logistic regression analysis. Model 1 was constructed based on the density at a threshold of 0.6 and the APACHE III score, while model 2 was derived using the density at a threshold of 0.6 and the SOFA score. When comparing the predictive accuracy of density at a 0.6 threshold alone with a predictive method that incorporates both density at a 0.6 threshold and the APACHE III score, the latter demonstrated a higher AUC (0.951; 95% CI, 0.893–1.000) for predicting good outcome. This predictive accuracy was significantly higher than density at the 0.6 threshold ($P = 0.04$) alone, or tended to be higher than APACHE III score alone ($P = 0.09$). This improvement in predictive accuracy enhanced the efficacy of the model for predicting SAE outcomes (Fig. 2A). Moreover, a higher APACHE III score and lower density values at the 0.6 threshold were indicative of poor outcomes. Conversely, higher density values at a 0.6 threshold, even in conjunction with higher APACHE III scores, were linked to good outcomes, as indicated by the connectivity analysis (Fig. 3). The logistic regression formula used to predict the likelihood of a good outcome was as follows:

	Univariate analysis		Model 1 (Density 0.6 & APACHE III)		Model 2 (Density 0.6 & SOFA)	
	OR (95% CI)	*P*‡	OR (95% CI)	*P*‡	OR (95% CI)	*P*‡
Density 0.6 (per 0.1 unit increase)	2.71 (1.10–6.67)	0.03	5.05 (1.28–19.84)	0.02	4.31 (0.93–19.83)	0.06
APACHE III (10 unit increase)	0.59 (0.43–0.81)	0.001	0.47 (0.29–0.75)	0.001		
SOFA (1 unit increase)	0.62 (0.47–0.81)	0.001			0.60 (0.43–0.82)	0.001
AUC (95% CI)						
Density 0.6 (per 0.1 unit increase)	0.72 (0.56–0.88)					
APACHE III (10 unit increase)	0.86 (0.73–0.98)					
SOFA (1 unit increase)	0.89 (0.79–0.99)					
Model 1 (Density 0.6 & APACHE III)			0.95 (0.89–1.00)			
Model 2 (Density 0.6 & SOFA)					0.94 (0.87–1.00)	

Table 4. Prediction model of good outcome based on connectivity analysis and sepsis severity. OR: odds ratio; APACHE II: Acute Physiology And Chronic Health Evaluation III; SOFA: Sequential Organ Failure Assessment. †*P*-value by logistic regression using Firth's penalized maximum likelihood method.

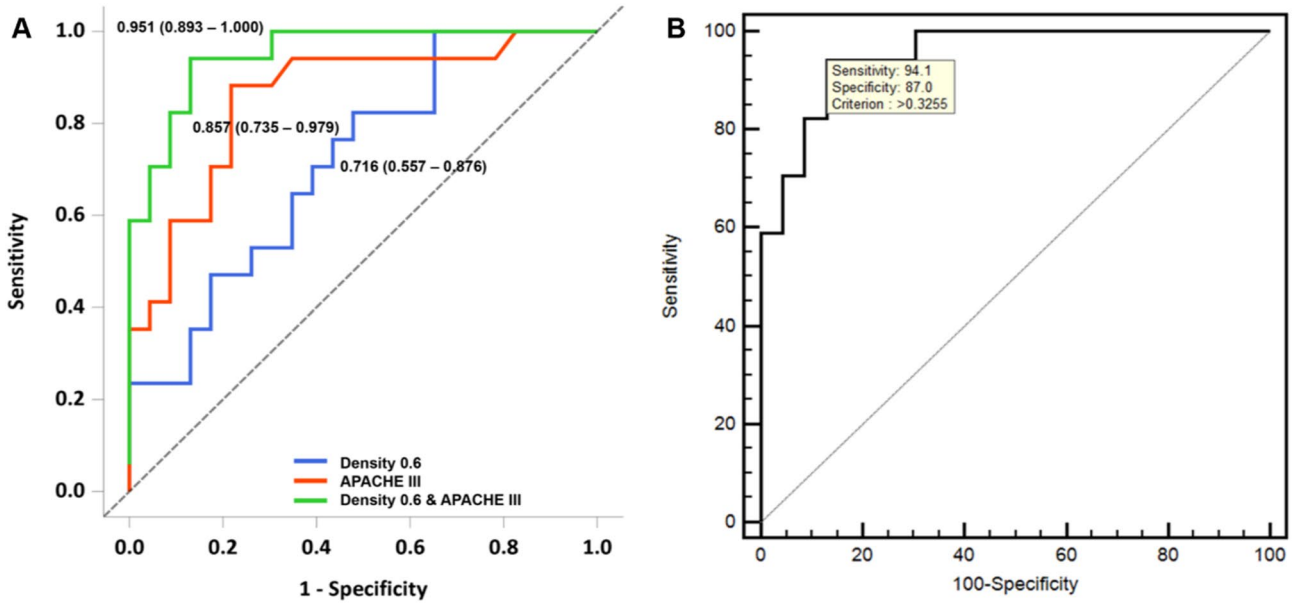

Fig. 2. Receiver operating characteristic curves depicting the prediction of outcomes following SAE. This plot demonstrates the correlation between sensitivity (Y-axis) and the reciprocal of specificity (X-axis), highlighting the highest area under the curve (AUC) for Acute Physiology and Chronic Health Evaluation (APACHE) III with a density of 0.6 and a composite of APACHE III with a density of 0.6. The use of both APACHE III and density at 0.6 resulted in the highest AUC value (0.951 [0.893–1.000]), outperforming AUC values obtained when using APACHE III alone (0.857 [0.735–0.979]) or density at 0.6 alone (0.716 [0.557–0.876]). (**A**) Notable variances observed between the combined approach and each individual predictor (APACHE III with density at 0.6 vs. density of 0.6, $P = 0.04$; APACHE III with density vs. APACHE III, $P = 0.09$); (**B**) Cutoff values of predictive methods with sensitivity and specificity.

$$\Pr(Y = good) = \frac{1}{1 + \exp(-3.1822 - 16.1861 \times density\,at\,0.6 + 0.0760 \times APACHE\,III)}$$

The optimal threshold value for predicting good outcomes in SAE was 0.3255, yielding a sensitivity of 94.1% and specificity of 87.0% based on the Youden index. A value > 0.3255 in this equation signified an increased likelihood of a good outcome (Fig. 2B).

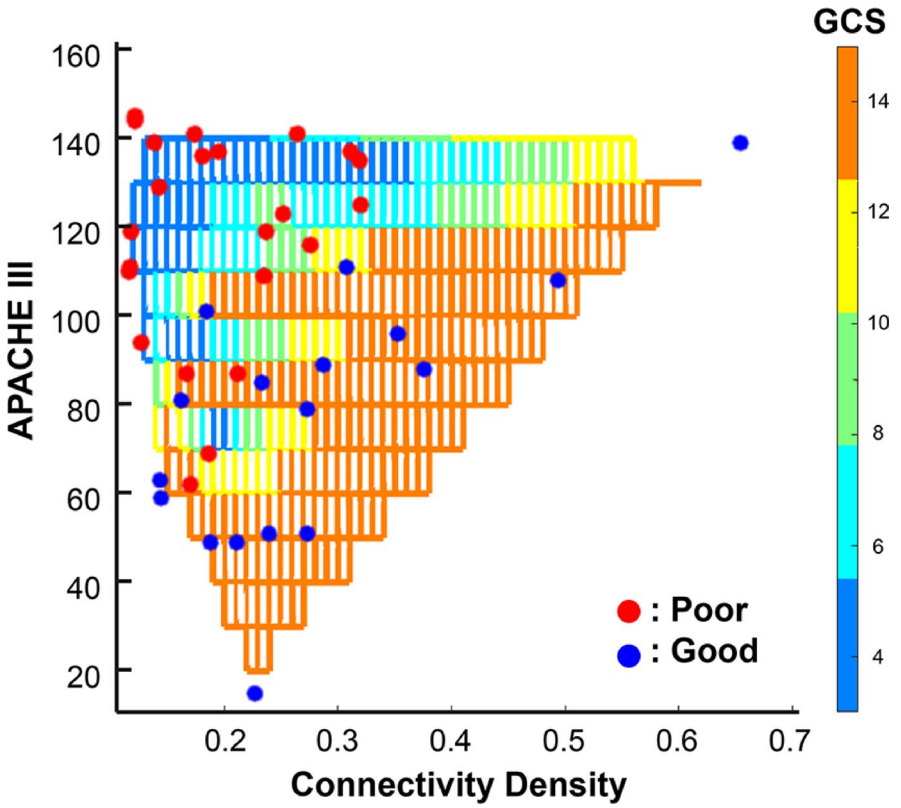

Fig. 3. Three-dimensional mesh plot of the prediction method. Correlation between Acute Physiology and Chronic Health Evaluation (APACHE) III and connectivity density (threshold = 0.6) with outcomes after sepsis-associated encephalopathy (SAE). Visualization was performed after SAE in patients with an average age of 70.8 years (n = 40); 17 patients had good outcomes after SAE. Discretely color-coded mesh (blue to orange) representing Glasgow Coma Scale scores from 0 to 15 correlated with the connectivity density threshold at 0.6 and APACHE III score (Y-axis) using natural neighbor interpolation. Acquired data points are represented by red and blue square dots, indicating poor (n = 23) and good (n = 17) outcomes, respectively. Higher APACHE III scores and lower connectivity densities were associated with poorer outcomes. Although the APACHE III score increased, a higher connectivity density value of the connectivity analysis was associated with a good outcome.

Discussion

In this study, we demonstrated that higher prefrontal functional connectivity, as assessed using oxyhemoglobin oscillations, was associated with favorable outcomes in SAE. Moreover, we developed a predictive model for favorable outcomes by incorporating the density value of the connectivity analysis and the APACHE III score.

SAE is a complex condition that arises in response to infection and may result in brain dysfunction in patients with sepsis. The mechanisms underlying brain dysfunction in SAE have not yet been fully elucidated. However, neuroinflammatory responses and ischemia play key roles in neuronal function, even in the absence of a direct invasion of infectious agents to central nervous system. Other suggested mechanisms include microscopic brain injury, BBB dysfunction, and cerebral microcirculation impairment leading to ischemia, vascular complex dysfunction, impaired neurovascular coupling, disrupted neurotransmission, and alterations in brain metabolism due to oxidative stress and inflammatory responses. These responses can potentially alter neuronal function, vitality, and connectivity in the central nervous system[6,8–11,22,42,43].

Diagnosing and predicting outcomes of SAE remain challenging. The diagnostic process relies on clinical assessments and the exclusion of other potential causes of changes in mental state[7–9,22]. The severity and outcomes of SAE are influenced by the severity of sepsis and intensive care for patients with sepsis. SAE prognosis correlates with the severity of sepsis and efficacy of antibiotic treatment[44–46]. Moreover, electrophysiological studies, including electroencephalography and somatosensory evoked potential, have been recognized as valuable tools in identifying patients with SAE[7,46–48]. However, no tools are available for predicting outcomes of patients with SAE.

Brain connectivity assessments using fNIRS based on graph theoretical approaches can assess the integrity and synchronous functional activity of brain regions and quantify relationships in neuronal networks[35,49]. Functional connectivity analysis, such as the prefrontal correlation coefficients of oxyhemoglobin, was performed for three properties: density, clustering coefficient, and global efficiency. Density and global efficiency are interconnected with the global connectivity of brain networks[20,35,35]. Previous studies have shown a positive association between higher oxyhemoglobin correlation coefficients and improved connectivity[15,20,35,36]. In the

present study, significantly lower connectivity values were observed in the group with poor outcomes, suggesting compromised neural synchronization and potentially diminished functional connectivity in the brain following SAE. Therefore, connectivity analysis values of oxyhemoglobin may serve as indicators of brain dysfunction associated with SAE.

Furthermore, a predictive model was formulated to evaluate outcomes following SAE by incorporating the APACHE III score and density values derived from connectivity analysis. The APACHE III score comprises a range of parameters, including physiological variables, vital signs, urine output, neurological scores, age, and comorbid conditions. It is used to assess the severity of medical conditions that can significantly influence the outcomes of patients with sepsis and SAE[25,44,50–52]. However, the reliability of APACHE III as the sole predictor is limited as it primarily reflects the severity of systemic infection without directly evaluating brain dysfunction. Furthermore, there remains a lack of adequate methodology to assess brain function for predicting neurological outcomes in patients with SAE[7–9,45–48,53]. In contrast, our model, which integrates both APACHE III and density values, exhibited markedly enhanced accuracy in forecasting neurological outcomes through brain connectivity analysis, presenting distinct advantages over conventional methods.

This study had some limitations. First, the sample size was relatively small as this was a pilot study. Furthermore, a validation study was not conducted in independent groups. However, the power of the predictive model in forecasting good outcomes was superior to that of APACHE III or density values alone. External validation of this model warrants further investigation. Second, the minimum duration of NIRSIT monitoring was approximately 300 s, which may not have been long enough to adequately capture functional connectivity. However, in our experience, a minimum of 5 min of monitoring was adequate to assess brain connectivity, except for limitations in very low frequency oscillations[15]. Third, we assessed neurological outcomes at discharge, which may have been too short to accurately evaluate outcomes. Fourth, we included patients with sepsis who were referred to neurointensivists for a comprehensive neurological evaluation; consequently, there may be a selection bias of the study.

In conclusion, our study demonstrated that the incorporation of connectivity analysis using oxyhemoglobin in our predictive model can reliably predict favorable neurological outcomes at discharge in patients with SAE in this preliminary study. This methodology has the potential to be a valuable resource for guiding future clinical decisions for patients with SAE. Furthermore, our predictive method serves as a prognostic tool, emphasizing the importance of quantitative evaluation and the ability to predict outcomes. This warrants further investigation for wider applicability and allocation of sufficient resources. To improve the predictive ability of our model, it is essential to conduct comprehensive multicenter studies that involve prolonged and repeated monitoring using fNIRS, which is crucial for external validation and to confirm the prognostic accuracy of the model.

Data availability

To inquire access to the study data, contact the corresponding author (Sang-Bae Ko).

Received: 7 June 2024; Accepted: 15 May 2025
Published online: 23 May 2025

References

1. Czajka, S. et al. Validation of APACHE II, APACHE III and SAPS II scores in in-hospital and one year mortality prediction in a mixed intensive care unit in Poland: A cohort study. *BMC Anesthesiol.* **20**, 1–8 (2020).
2. Vincent, J.-L. et al. Use of the SOFA score to assess the incidence of organ dysfunction/failure in intensive care units: Results of a multicenter, prospective study. *Crit. Care Med.* **26**, 1793–1800 (1998).
3. Singer, M. et al. The third international consensus definitions for sepsis and septic shock (Sepsis-3). *JAMA* **315**, 801–810 (2016).
4. Dono, A., Esquenazi, Y. & Choi, H. A. Gut microbiome and neurocritically ill patients. *J. Neurocritical Care* **15**, 1–11 (2022).
5. Baik, S. M. et al. Validation of presepsin measurement for mortality prediction of sepsis: a preliminary study. *Acute Crit. Care* **37**(4), 527–532 (2022).
6. Sonneville, R. et al. The spectrum of sepsis-associated encephalopathy: A clinical perspective. *Crit. Care* **27**(1), 386 (2023).
7. Mazeraud, A. et al. Septic-associated encephalopathy: A comprehensive review. *Neurotherapeutics* **17**(2), 392–403 (2020).
8. Gofton, T. E. & Young, G. B. Sepsis-associated encephalopathy. *Nat. Rev. Neurol.* **8**(10), 557–566 (2012).
9. Chaudhry, N. & Duggal, A. K. Sepsis associated encephalopathy. *Adv. Med.* **2014**, 762320 (2014).
10. Ren, C. et al. Sepsis-associated encephalopathy: A vicious cycle of immunosuppression. *J. Neuroinflammation* **17**(1), 14 (2020).
11. Ito, H. et al. Sepsis-Associated Encephalopathy: A mini-review of inflammation in the brain and body. *Front. Aging Neurosci.* **27**(14), 912866 (2022).
12. Papadopoulos, M. C. et al. Pathophysiology of septic encephalopathy: A review. *Crit. Care Med.* **28**(8), 3019–3024 (2000).
13. Jung, J.-M. et al. New directions in infection-associated ischemic stroke. *J. Clin. Neurol.* **20**(2), 140–152 (2024).
14. Bolton, C. F., Young, G. B. & Zochodne, D. W. The neurological complications of sepsis. *Ann. Neurol.* **33**(1), 94–100 (1993).
15. Kim, T. J. et al. Prognostication of neurological outcome after cardiac arrest using wavelet phase coherence analysis of cerebral oxygen. *Resuscitation* **150**, 41–49 (2020).
16. Yücel, M. A. et al. Best practices for fNIRS publications. *Neurophotonics* **8**(1), 012101 (2021).
17. Ruan, N. et al. Cortical activation in elderly patients with Alzheimer's disease dementia during working memory tasks: a multichannel fNIRS study. *Front. Aging Neurosci.* **25**(16), 1433551 (2024).
18. Ueda, S. et al. Reduced prefrontal hemodynamic response in adult attention-deficit hyperactivity disorder as measured by near-infrared spectroscopy. *Psychiatry Clin. Neurosci.* **72**(6), 380–390 (2018).
19. Dong, S.-Y. et al. Prefrontal functional connectivity during the verbal fluency task in patients with major depressive disorder: A functional near-infrared spectroscopy study. *Front. Psychiatry.* **21**(12), 659814 (2021).
20. Fox, M. D. & Greicius, M. Clinical applications of resting state functional connectivity. *Front. Syst. Neurosci.* **17**(4), 19 (2010).
21. Liu, Y. et al. Detecting residual brain networks in disorders of consciousness: A resting-state fNIRS study. *Brain Res.* **1**(1798), 148162 (2023).
22. Iacobone, E. et al. Sepsis-associated encephalopathy and its differential diagnosis. *Crit. Care Med.* **37**(10 Suppl), S331–S336 (2009).
23. Cope, M. & Delpy, D. T. System for long-term measurement of cerebral blood and tissue oxygenation on newborn infants by near infra-red transillumination. *Med. Biol. Eng. Comput.* **26**(3), 289–294 (1988).

24. Keegan, M. T. et al. APACHE III outcome prediction in patients admitted to the intensive care unit after liver transplantation: a retrospective cohort study. *BMC Surg.* **29**(9), 11 (2009).
25. Knaus, W. A. et al. The APACHE III prognostic system: Risk prediction of hospital mortality for critically III hospitalized adults. *Chest* **100**, 1619–1636 (1991).
26. Park, H., Lee, J., Oh, D. K. et al. Investigators KSA. Serial evaluation of the serum lactate level with the SOFA score to predict mortality in patients with sepsis. *Sci. Rep. 13*(1), 6351 (2023).
27. Jain, S. & Iverson. L. M. Glasgow coma scale (2018).
28. Gonçalves, B. et al. Incidence and impact of sepsis on long-term outcomes after subarachnoid hemorrhage: A prospective observational study. *Ann. Intensive Care* **20**(9), 94 (2019).
29. Bindra, J. et al. Is impaired cerebrovascular autoregulation associated with outcome in patients admitted to the ICU with early septic shock?. *Crit. Care Resusc.* **18**(2), 95–101 (2016).
30. Kim, J.-M. et al. Assessment of cerebral autoregulation using continuous-wave near-infrared spectroscopy during squat-stand maneuvers in subjects with symptoms of orthostatic intolerance. *Sci. Rep.* **8**(1), 13257 (2018).
31. OBELAB Inc. (2022). NIRSIT Channel Information. Seoul. Available online at: https://www.obelab.com/info/notice.php
32. Cooper, R. J. et al. A systematic comparison of motion artifact correction techniques for functional near-infrared spectroscopy. *Front. Neurosci.* **11**(6), 147 (2012).
33. Brigadoi, S. et al. Motion artifacts in functional near-infrared spectroscopy: A comparison of motion correction techniques applied to real cognitive data. *Neuroimage* **85**, 181–191 (2014).
34. Siddiquee, M. R. et al. Movement artefact removal from NIRS signal using multi-channel IMU data. *Biomed. Eng.* **17**(1), 120 (2018).
35. Liao, X., Vasilakos, A. V. & He, Y. Small-world human brain networks: perspectives and challenges. *Neurosci. Biobehav. Rev.* **77**, 286–300 (2017).
36. Racz, F. S. et al. Increased prefrontal cortex connectivity during cognitive challenge assessed by fNIRS imaging. *Biomed. Opt. Express* **8**(8), 3842–3855 (2017).
37. Rubinov, M. & Sporns, O. Complex network measures of brain connectivity: Uses and interpretations. *Neuroimage* **52**(3), 1059–1069 (2010).
38. Novi, S. L. et al. Resting state connectivity patterns with near-infrared spectroscopy data of the whole head. *Biomed. Opt. Express* **7**(7), 2524–2537 (2016).
39. Racz, F. S., Mukli, P., Nagy, Z. & Eke, A. Increased prefrontal cortex connectivity during cognitive challenge assessed by fNIRS imaging. *Biomed. Opt. Express* **8**(8), 3842–3855 (2017).
40. Youden, W. J. Index for rating diagnostic tests. *Cancer* **3**(1), 32–35 (1950).
41. DeLong, E. R., DeLong, D. M. & Clarke-Pearson, D. L. Comparing the areas under two or more correlated receiver operating characteristic curves: a nonparametric approach. *Biometrics* **44**(3), 837–45.33 (1988).
42. Póvoa, P. et al. How to use biomarkers of infection or sepsis at the bedside: Guide to clinicians. *Intensive Care Med.* **49**(2), 142–153 (2023).
43. Stubbs, D. J., Yamamoto, A. K. & Menon, D. K. Imaging in sepsis-associated encephalopathy—Insights and opportunities. *Nat. Rev. Neurol.* **9**(10), 551–561 (2013).
44. Luo, H. et al. Association between the first 24 hours $PaCO_2$ and all-cause mortality of patients suffering from sepsis-associated encephalopathy after ICU admission: A retrospective study. *PLoS ONE* **18**(10), e0293256 (2023).
45. Liu, Y. et al. Development and validation of a predictive model for in-hospital mortality in patients with sepsis-associated liver injury. *Ann. Transl. Med.* **10**(18), 997 (2022).
46. Helmy, T. A. et al. EEG changes in critically ill patients with sepsis associated encephalopathy and its correlation with morbidity and mortality. *Alex. J. Med.* **60**, 11–16 (2024).
47. Feng, Q. et al. Characterization of sepsis and sepsis-associated encephalopathy. *J. Intensive Care Med.* **34**(11–12), 938–945 (2019).
48. Orhun, G. et al. Clinical and electroencephalographic findings in patients with sepsis-associated encephalopathy and the evaluation of their effects on survival. *Eur. Arch. Med. Res.* **36**(1), 73–82 (2020).
49. Euler, L. Solutio problematis ad geometriam situs pertinentis. Commentarii academiae scientiarum Petropolitanae. 1741, 128–140.
50. Zhao, L. et al. Mechanical learning for prediction of sepsis-associated encephalopathy. *Front. Comput. Neurosci.* **16**(15), 739265 (2021).
51. Zhao, Q. et al. The nomogram to predict the occurrence of sepsis-associated encephalopathy in elderly patients in the intensive care units: A retrospective cohort study. *Front. Neurol.* **2**(14), 1084868 (2023).
52. Mei, J. et al. Optimizing the prediction of sepsis-associated encephalopathy with cerebral circulation time utilizing a nomogram: A pilot study in the intensive care unit. *Front. Neurol.* **11**(14), 1303075 (2024).
53. de Araújo, B. E. S. et al. Clinical features, electroencephalogram, and biomarkers in pediatric sepsis-associated encephalopathy. *Sci. Rep.* **12**(1), 10673 (2022).

Author contributions

S-B K., and TJ K. contributed to the study concept and design. TJ K., J C., JS Lee, J-M K., and H-M B. contributed to data analysis. TJ K. and S-H P. contributed to data collection. TJ K., J-M K., and S-B-K. drafted the manuscript. All authors read and approved the manuscript.

Funding

This work was funded by Seoul National University Hospital (No. 0320210350). The funding organizations had no role in the study or the preparation of this report.

Declarations

Competing interests

The authors declare no competing interests.

Additional information

Supplementary Information The online version contains supplementary material available at https://doi.org/10.1038/s41598-025-02658-9.

Correspondence and requests for materials should be addressed to S.-B.K.

Reprints and permissions information is available at www.nature.com/reprints.